

Shape-Selective Alkylation of Biphenyl over H-[Al]-SSZ-24 Zeolites with AFI Topology

Akira Ito, Hiroyoshi Maekawa, Hiroaki Kawagoe, Kenichi Komura, Yoshihiro Kubota,† and Yoshihiro Sugi*

Department of Materials Science and Technology, Faculty of Engineering, Gifu University, Gifu 501-1193

Received June 23, 2006; E-mail: ysugi@cc.gifu-u.ac.jp

H-[Al]-SSZ-24 zeolites with AFI topology were synthesized through the alumination of [B]-SSZ-24 zeolites, and applied for the alkylation of biphenyl (BP). H-[Al]-SSZ-24 zeolites have high activity for the isopropylation. The shape-selective formation of 4,4′-diisopropylbiphenyl (4,4′-DIPB) occurred at moderate temperature; however, the selectivity for 4,4′-DIPB decreased with an increase in the reaction temperature. Isomerization of 4,4′-DIPB occurred at higher temperatures over internal and external acid sites when there are enough acid sites inside the channels. The channels can discriminate 4,4′-DIPB from the other DIPB isomers in their transition states; however, they can not prevent the isomerization of 4,4′-DIPB at higher temperatures. The selectivity for the least bulky 4,4′-dialkylbiphenyl increased with the bulkiness of alkylating agents in the order: isopropylation < *s*-butylation < *t*-butylation. These results strongly support the shape-selective formation of the least bulky products inside the channels of H-[Al]-SSZ-24 zeolites.

Zeolites are the most promising microporous crystals for achieving highly shape-selective catalysis because their pores are uniformly distributed and have dimensions allowing both organic reactants and products to enter, to accommodate, and to leave.[1,2] Large-pore molecular sieves (LPMS) are expected to be useful as catalysts in the alkylation of polynuclear aromatics.[3–5] 4,4′-Diisopropylbiphenyl (4,4′-DIPB) has been selectively produced from biphenyl (BP) over dealuminated H-mordenite (MOR).[3–9] It is very interesting to elucidate the catalytic features of LPMS pores in the catalysis; however, there have been very few articles on the subject other than MOR. Our previous relevant findings on the subjects have been published on the alkylation of BP over H-[Al]-SSZ-31,[10] H-[Al]-CIT-5,[11] SAPO-5,[12] and MAPO-5 (M: Mg, Ca, Sr, Ba, and Zn).[13–15]

H-[Al]-SSZ-24 zeolite is a high-silica large-pore molecular sieve, which is isostructural with $AlPO_4$-5 (AFI topology),[16] and is expected to work as a potential catalyst for shape-selective alkylation of polynuclear aromatics because of its straight twelve-membered ring (12-MR) channel structure. SSZ-24 zeolite was first synthesized by Zones as its pure-silica form using 1-trimethylammonioadamantane as a structure-directing agent (SDA).[17] [B]-SSZ-24 zeolite in borosilicate version was subsequently synthesized using a calcined form of boron-substituted zeolite beta ([B]-BEA) as the boron and silicon sources.[18] Lobo and Davis reported the synthesis of [B]-SSZ-24 zeolite using *N*(16)-methylsparteinium ($MeSPA^+$) as SDA and using sodium borate as the source of boron.[19] [B]-SSZ-24 zeolite was easily converted to H-[Al]-SSZ-24 zeolites by post-synthetic treatment with aluminum nitrate.[19] This isomorphous substitution will be expressed as "alumination" in this paper.

† Present address: Department of Materials Science and Engineering, Graduate School of Engineering, Yokohama National University, Yokohama 240-8501

It is important to know how zeolite structure influences shape-selective character of the alkylation of BP and how the bulkiness of alkylating agent influences shape-selective catalysis. These questions have led us to investigate the catalytic properties of H-[Al]-SSZ-24 zeolites. In this paper, we describe the isopropylation, *s*-butylation, and *t*-butylation of BP over H-[Al]-SSZ-24 zeolites to elucidate the relationships between their pore structure and shape-selective catalysis.

Experimental

Synthesis of H-[Al]-SSZ-24 Zeolites. *N*(16)-Methylsparteinium hydroxide ($[MeSPA^+]OH^-$) was synthesized by the quaternization of sparteine with methyl iodide, followed by ion-exchange with ion-exchange resin. The detailed procedure is reported elsewhere.[20] [B]-SSZ-24 was hydrothermally synthesized from a gel having the composition $1.0SiO_2$–$0.04B_2O_3$–$0.2[MeSPA^+]OH^-$–$0.1NaOH$–$50H_2O$.[19] A typical procedure is as follows. After stirring the mixture of a NaOH solution (32 wt %, 375 mg), a $[MeSPA^+]OH^-$ solution (0.700 mmol g^{-1}, 14.3 g), and sodium borate decahydrate ($Na_2B_4O_7 \cdot 10H_2O$, 381 mg) until the solution became clear, and then, 3.00 g of fumed silica (Cab-O-Sil M-5, Cabot) and 33.0 g of de-ionized water were added to the homogeneous mixture. A small amount (60 mg) of [B]-BEA seed was added to the mixture, which was further stirred for 3 h. The mixture was then transferred to a 23-mL Teflon-lined stainless autoclave. The autoclave was kept statically in a convection oven at 175 °C for 5 days. The crystals were collected by filtration, washed several times with de-ionized water, and dried overnight.

To remove the organic SDA occluded inside the [B]-SSZ-24 zeolite, the as-synthesized sample was kept in a muffle furnace, and heated stepwise in a flow of air (100 mL min^{-1}). The temperature was raised from room temperature to 650 °C over a period of 310 min, and maintained at the same temperature for 4 h. Finally, the calcined sample was cooled to room temperature under ambient conditions.

[B]-SSZ-24 zeolite was aluminated to H-[Al]-SSZ-24 zeolites

Published on the web January 12, 2007; doi:10.1246/bcsj.80.215

Table 1. Properties of H-[Al]-SSZ-24 Zeolites

	SiO_2/B_2O_3	SiO_2/Al_2O_3	Surface area /$m^2\,g^{-1}$	Pore volume /$cm^3\,g^{-1}$	*h*-Peak /°C	Acid amount /mmol g^{-1}
[B]-SSZ-24	71	—	379	0.16	—	—
A_1	816	768	357	0.14	243	0.024
A_3	—	172	340	0.13	278	0.165
A_5	—	135	350	0.15	269	0.175

by heating in an aluminum nitrate solution at 80 °C for 18 h. The relative weight of components in this alumination process was zeolite:$Al(NO_3)_3$:H_2O = 1:1:50, and this process was repeated several times.

Catalytic Reaction. The alkylation of BP was carried out in a 100-mL SUS-316 autoclave under a pressure of the alkylating agent. Typical conditions of the isopropylation are: BP 50 mmol, zeolite 0.25 g, propene pressure 0.8 MPa, reaction temperature 150–250 °C, and reaction time 4 h. An autoclave containing BP and the zeolite was purged with N_2 before heating. After reaching the reaction temperature, propene was introduced to the autoclave, and the pressure kept constant throughout the reaction. After cooling the autoclave, the zeolite was filtered off, and bulk products were diluted with toluene. The products were analyzed by gas chromatography (GC-14A, Shimadzu Corporation, Kyoto) equipped with an Ultra-1 capillary column (25 m × 0.2 mm; Agilent Technologies, MA, U.S.A.), and identified by using a Shimadzu Gas Chromatograph-Mass Spectrometer GC-MS 5000. The yield of each product was calculated on the basis of the amounts of starting BP, and the selectivities for each IPBP and DIPB isomers are expressed based on the total amounts of IPBP and DIPB isomers, respectively.

$$\text{Selectivity for a DIPB (IPBP) isomer (\%)} = \frac{\text{Each DIPB (IPBP) isomer (mol)}}{\text{DIPB (IPBP) isomers (mol)}} \times 100. \quad (1)$$

The analysis of products encapsulated in the zeolite used for the reaction was carried out as follows. The zeolite was filtered off, washed well with 200 mL of acetone, and dried at 110 °C for 12 h. The zeolite (100 mg) was carefully dissolved in 47% aqueous hydrofluoric acid (3 mL) at room temperature. The solution was basified with solid potassium carbonate, and the organic layer was extracted three times with 20 mL of dichloromethane with ice-cooling. After removal of the solvent in vacuo, the residue was dissolved in 5 mL of toluene, and 10 mg of naphthalene was added as an internal standard. GC analysis was performed according to the same procedure as that for bulk products. The encapsulated products were expressed by the selectivity because quantitative analysis was difficult.

The *s*- and *t*-butylations of BP were carried out in a similar manner as the isopropylation.

Characterization of Zeolites. The crystal structure of zeolites was determined by powder X-ray diffraction using Shimadzu XRD-6000 with Cu Kα radiation ($\lambda = 0.15418$ nm). Elemental analysis was performed by inductive coupled plasma atomic emission spectroscopy on a JICP-PS-1000 UV (Teledyne Leeman Labs Inc., NH, U.S.A.). Crystal size and morphology were observed by using an S-4300 FE-SEM microscope (Hitachi Corporation, Tokyo). Nitrogen adsorption measurements were carried out on a Belsorp 28SA (BEL Japan Inc., Osaka). Temperature-programmed desorption of ammonia (NH_3-TPD) was measured using a Bel TPD-66 apparatus. The zeolite was evacuated at 400 °C for 1 h, and ammonia was adsorbed at 100 °C followed by further evacuation for 1 h. Then, the sample was heated from 100 to 710 °C at a rate of 10 °C min^{-1} in a helium stream. TG analysis was performed on a Shimadzu DTG-50 analyzer with temperature-programmed rate of 10 °C min^{-1} in an air stream. The solid ^{11}B, ^{29}Si, and ^{27}Al NMR spectra were recorded at room temperature under magic-angle spinning (MAS) by using 7.0 mm diameter zirconia rotor spinning at 4 kHz on an Inova 400 spectrometer (Varian Corporation, MA, U.S.A.).

Results and Discussion

Properties of H-[Al]-SSZ-24 Zeolites. [B]-SSZ-24 zeolites were synthesized by the methods in the literature.[20] Typical properties of the zeolites are shown in Table 1. [B]-SSZ-24 zeolite was converted from [B]-BEA using ($MeSPA^+$)OH^- as the SDA under hydrothermal conditions. [B]-SSZ-24 zeolite had a SiO_2/B_2O_3 ratio of 71, specific surface area (379 $m^2\,g^{-1}$), and pore volume (0.16 $cm^2\,g^{-1}$). H-[Al]-SSZ-24 zeolites were obtained from [B]-SSZ-24 by repeating the alumination process as described in the Experimental Section.[18] Samples aluminated for *n* times are abbreviated as A_n (*n*: 1–8). Figure 1 shows the influences of the boron and aluminum contents on the alumination. Boron content of [B]-SSZ-24 zeolite decreased rapidly due to alumination; however, the aluminum content gradually increased with each repetition. From these samples, we chose samples, A_1, A_3, and A_5 of which the SiO_2/Al_2O_3 ratios were 768, 172, and 135, respectively.

Figure 2 shows the XRD patterns of calcined [B]-SSZ-24 and H-[Al]-SSZ-24 zeolites A_1, A_3, and A_5. Figure 3 shows

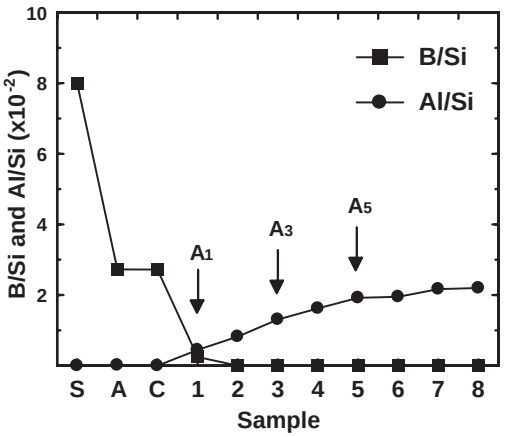

Fig. 1. The isomorphous substitution of boron in [B]-SSZ-24 zeolites with aluminum. Abbreviation: S: starting gel; A: as-synthesized sample; C: calcined sample; Arabic numerals: numbers 1–8 correspond to the sample A_1–A_8, respectively as defined in the text. A_1, A_3, and A_5 were used for the catalysis.

SEM images of [B]-SSZ-24 and H-[Al]-SSZ-24 zeolites A_1, A_3, and A_5. These results show that the structures of H-[Al]-SSZ-24 zeolites were retained during the alumination.

NH_3-TPD spectra of H-[Al]-SSZ-24 zeolites are shown in Fig. 4. They have two types of desorption peak, so-called *l*- and *h*-peaks, at 160–180 and 260–280 °C, respectively. The *h*-peak is due to desorbed NH_3 from Brønsted acidic sites, which work in solid acid catalysis. On the other hand, the *l*-peak is due to physisorbed NH_3, which plays no important role in solid acid catalysis. The acid amounts are 0.024, 0.165, and 0.175 mmol g^{-1} for A_1, A_3, and A_5 zeolites, respectively. These results show that the introduction of aluminum to nest silanol groups, formed by the deboronation, was almost saturated by the alumination for three times.

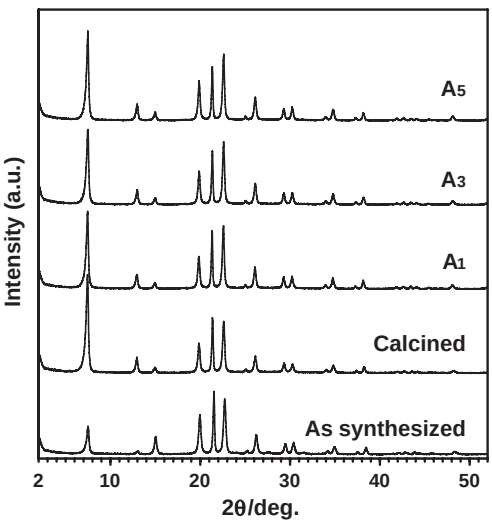

Fig. 2. XRD patterns of H-[Al]-SSZ-24 zeolites.

Figure 5 shows solid ^{11}B, ^{27}Al, and ^{29}Si MAS NMR spectra of H-[Al]-SSZ-24 zeolites during the alumination. ^{11}B MAS NMR spectra of as-synthesized [B]-SSZ-24 (not shown) gave only a peak at −3.7 ppm corresponding to tetrahedral boron. Upon calcination, a minor broad peak assignable to trigonal boron appeared at around 6.1 ppm[21] in addition to an intense, sharp peak at −3.7 ppm. The signals of these boron species almost disappeared after the first treatment with aluminum nitrate. The signals due to tetrahedral aluminum in the ^{27}Al MAS NMR spectra gradually developed during repeated alumination over three repetitions. The spectra were taken in

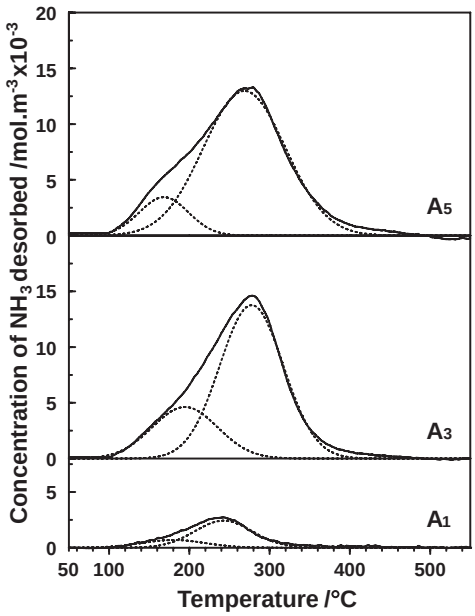

Fig. 4. NH_3-TPD profiles of H-[Al]-SSZ-24 zeolites.

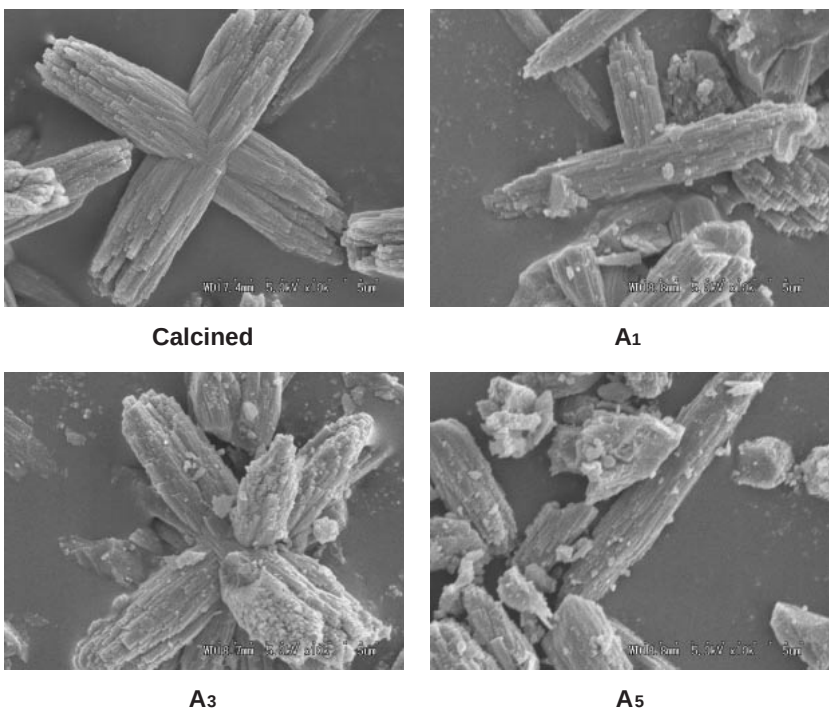

Fig. 3. SEM images of [B]-SSZ-24 and H-[Al]-SSZ-24 zeolites.

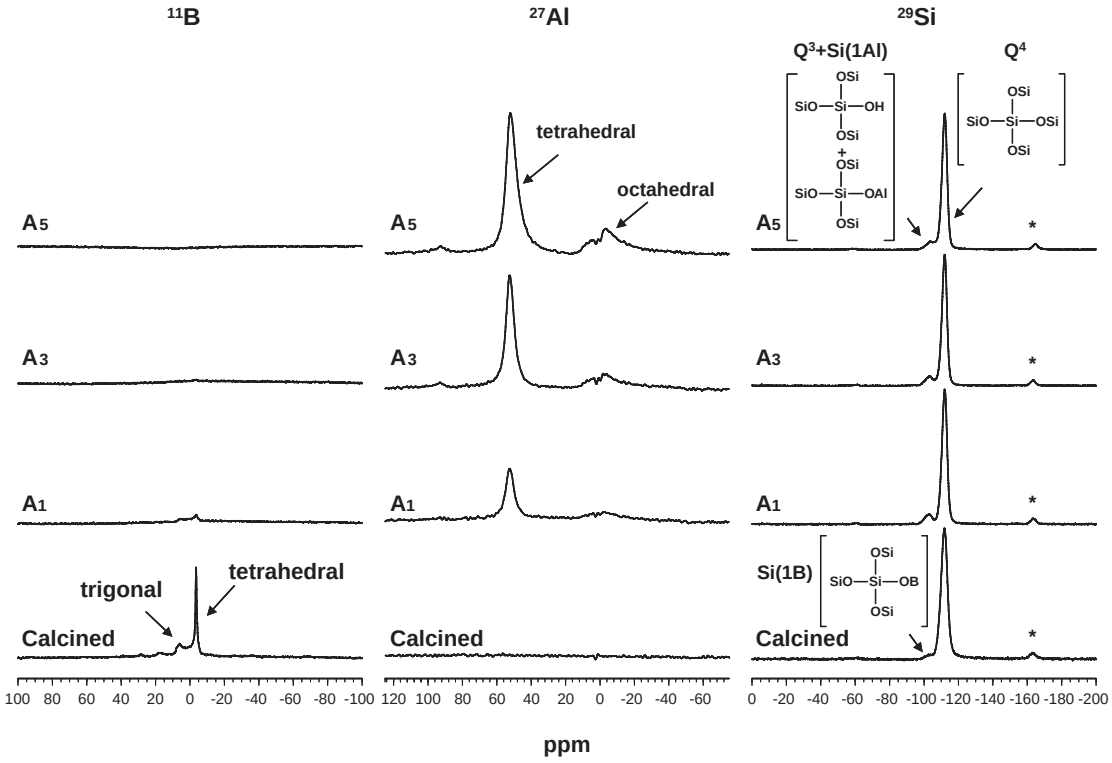

Fig. 5. Solid ^{11}B, ^{27}Al, and ^{29}Si MAS NMR spectra during the alumination of H-[Al]-SSZ-24 zeolites. * shows spinning side band peaks.

such a manner that the intensity reflects the amount. The major tetrahedral peaks were accompanied by minor octahedral peaks at an approximately constant ratio during the repeated aluminations. ^{29}Si MAS NMR spectra showed that the Q^4 species were predominant in all H-[Al]-SSZ-24 zeolites during the aluminations. Almost no Q^3 species was found in calcined [B]-SSZ-24 zeolite; however, small but significant amounts of the Q^3 species appeared in A_1 and A_3 zeolites. These results are consistent with the presence of residual silanol nests which are caused by the almost complete deboronation of [B]-SSZ-24 zeolite and a partial insertion of Al^{3+} into framework.

The Isopropylation of BP over H-[Al]-SSZ-24 Zeolites. Figure 6 shows the influence of reaction temperature on the products composition in the isopropylation of BP over A_1, A_3, and A_5 zeolites. [B]-SSZ-24 zeolite had no activity towards the isopropylation of BP at 250 °C; however, the isomorphous substitution of boron in [B]-SSZ-24 with aluminum enhanced the catalytic activity for the isopropylation. Particularly, A_3 and A_5 zeolites had very high activities affording isopropylbiphenyl (IPBP), diisopropylbiphenyl (DIPB), and triisopropylbiphenyl (TriIPB) isomers. These zeolites gave TriIPB in large amounts even at 200 °C. Catalytic activities of A_1 zeolite appeared at higher temperatures than those of A_3 and A_5 zeolites. However, the profiles of the yield of IPBP, DIPB, and TriIPB isomers over A_1 zeolite versus reaction temperature are quite resembled to A_3 and A_5 zeolites: the maximum yield of DIPB isomers over the A_3 and A_5 zeolites occurred about 300 °C higher than that of IPBP isomers of the A_1 zeolite. These results show that the isopropylation of BP proceeds through the consecutive mechanism. i.e., BP to IPBP, IPBP to DIPB, and DIPB to TriIPB, and that the channels of H-[Al]-SSZ-24 with relatively high amounts of acid such as A_3 and A_5 zeolites can enhance the formation of bulky TriIPB isomers. On the other hand, the formation of TriIPB isomers was quite negligible over H-MOR. These differences may be due to the slightly larger channels of H-[Al]-SSZ-24 zeolites compared to H-MOR.

The influence of SiO_2/Al_2O_3 ratio of H-[Al]-SSZ-24 zeolites on the catalytic activity and selectivity for 4,4′-DIPB are shown in Fig. 7. The activities appeared at low temperatures, such as 150 °C over A_3 and A_5 zeolites, and the conversion reached 100% at 225–250 °C. The selectivity for 4,4′-DIPB was around 70% at 150–225 °C, and it decreased with an increase in reaction temperature. A similar change in activity and selectivity were observed over A_1 zeolite, which has very small amount of acid sites. The catalytic activity appeared from 200 °C, and increased with the increase in reaction temperature. The selectivity for 4,4′-DIPB were around 75% at temperatures lower than 300 °C. The decrease in the selectivity occurred with the further increase in temperature. These high selectivities for 4,4′-DIPB in the level of 70–80% over A_1, A_3, and A_5 zeolites mean that the formation of 4,4′-DIPB occurred inside the channels of H-[Al]-SSZ-24 zeolites, and that the channels can discriminate 4,4′-DIPB from other isomers in the transition state. The difference in temperature for decreasing the selectivity is due to the acid amount in the zeolites, and not to the change of the pore structure of the zeolite.

The influences of reaction temperature on the selectivity for DIPB over A_3 and A_1 zeolites, which have SiO_2/Al_2O_3 ratio of 172 and 768, respectively, are also shown in Figs. 8 and 9. The selectivities for 4,4′-DIPB of bulk products were around 70% for both A_1 and A_3 zeolites: at the lower temperatures

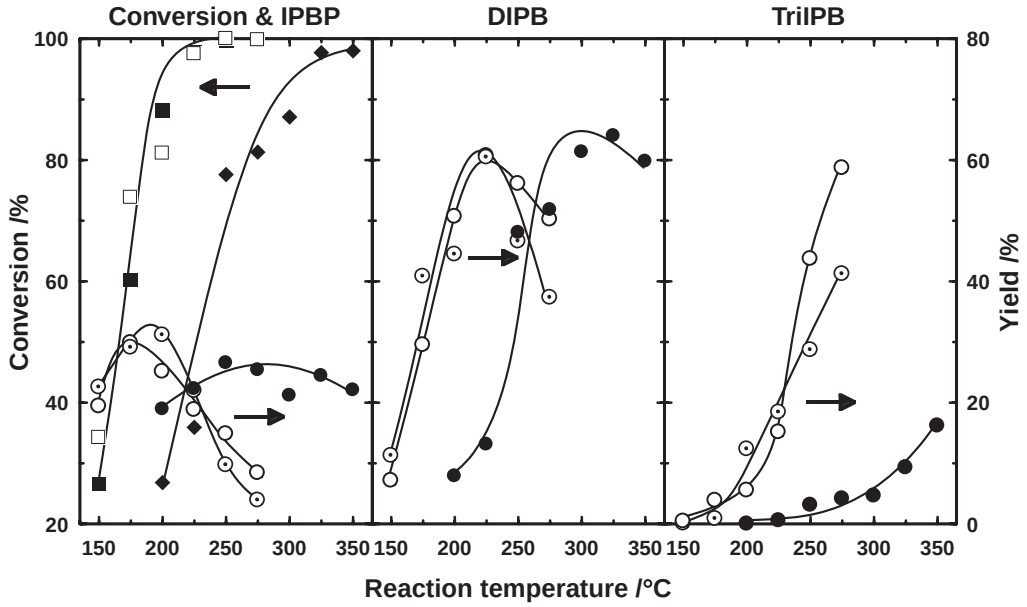

Fig. 6. The influence of alumination on catalytic activity and the selectivity for isopropylates in the isopropylation of BP over H-[Al]-SSZ-24 zeolites. Reaction conditions: zeolite (A_1, A_3, and A_5), 0.25 g; BP, 50 mmol; propene, 0.8 MPa; temperature, 150–275 °C; period, 4 h. Legends: conversion: ◆, A_1; ■, A_3; □, A_5. IPBP, DIPB, and TriIPB: ●, A_1; ○, A_3; ⊙, A_5.

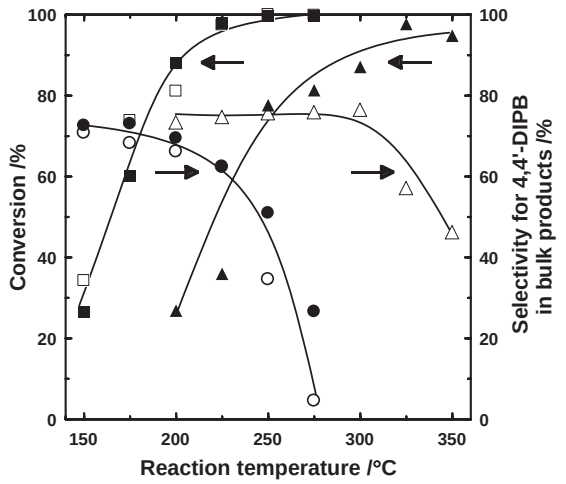

Fig. 7. The influence of alumination on the selectivity for 4,4′-DIPB in the isopropylation of BP over H-[Al]-SSZ-24 zeolites. Reaction conditions: see Fig. 6. Legends: conversion, ▲, A_1; ■, A_3; □, A_5. selectivity for 4,4′-DIPB, △, A_1; ●, A_3; ○, A_5.

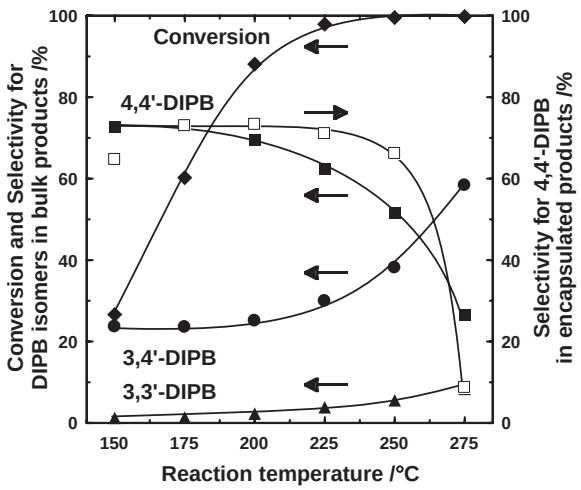

Fig. 8. The influence of reaction temperature on the selectivity for DIPB isomers in the isopropylation of BP over H-[Al]-SSZ-24 zeolite. Reaction conditions: zeolite: A_3, 0.25 g; BP, 50 mmol; propene, 0.8 MPa; temperature: 150–275 °C; period, 4 h.

than 200 °C for A_3 zeolite, and lower than 300 °C for A_1 zeolite. However, the selectivities of 4,4′-DIPB decreased with increasing reaction temperatures over both zeolites, and the selectivities for 3,4′-DIPB increased at higher temperatures. The decrease in the selectivity started at 225–250 °C for the A_3 zeolite, and at 300–325 °C for the A_1 zeolite. These results suggest that H-[Al]-SSZ-24 zeolites have high shape-selectivity for the isopropylation of BP at moderate temperatures, although it is lower than that of H-MOR as previously discussed.[3–8] However, quite different features were observed in the encapsulated products, i.e., the selectivity for 4,4′-DIPB in encapsulated products for A_3 zeolite was as high as those in bulk products below 250 °C, and it decreased rapidly at temperatures higher than 250 °C. These results means that isomerization of 4,4′-DIPB occurred over acid sites inside the channels and probably also at the external acid sites. On the other hand, the selectivity for 4,4′-DIPB for A_1 zeolite was as high as 70–80% even at higher temperatures, such as 300 °C, although the selectivity for 4,4′-DIPB in bulk products decreased at 325 °C. However, the selectivity for 4,4′-DIPB in encapsulated products were remained almost constant even at 325 °C. Therefore, the decrease in the selectivity for 4,4′-DIPB in bulk products over the A_1 zeolite is due to the isomerization at external acid sites. Thus, acid sites inside the channels of A_1 zeolite did not work as the catalysts of isomerization of 4,4′-DIPB because they have not enough amounts for the reaction. These

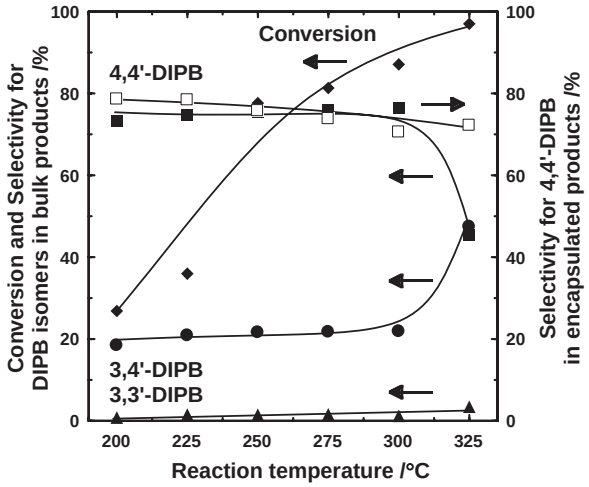

Fig. 9. The influence of reaction temperature on the selectivity for DIPB isomers in the isopropylation of BP over H-[Al]-SSZ-24 zeolite. Reaction conditions: zeolite: A_1, 0.25 g; BP, 50 mmol; propene, 0.8 MPa; temperature: 150–275 °C; period, 4 h.

results also show that the channels of SSZ-24 zeolite are large enough for the isomerization of 4,4′-DIPB and that the isomerization of 4,4′-DIPB occurred both at the external and internal acid sites although it depends on acid amounts. In contrast, no isomerization of 4,4′-DIPB occurred at the internal acid sites over H-MOR.[3–5]

These selectivities for 4,4′-DIPB of SSZ-24 zeolites are in the similar level to those of SAPO-5 and MAPO-5 molecular sieves with the AFI topology,[11,13–15] whereas the selectivity for 4,4′-DIPB is lower than those for H-MOR.[4–8] The differences in the selectivity for 4,4′-DIPB are due to the structural difference between H-MOR and molecular sieves with AFI topology.

The influence of reaction time on the selectivities for isopropylates in the isopropylation of BP over A_3 zeolite at 175 °C is shown in Fig. 10. The catalytic activity and the yield of isopropylates in the bulk products during the catalysis are shown in Fig. 10a. The yield of DIPB and TriIPB isomers increased with a decrease in that of the IPBP isomers. These results suggest the consecutive formation of isopropylates as discussed above. However, the selectivities for isopropylates in the encapsulated products shown in Fig. 10b indicate that the selectivities of isopropylates did not significantly vary during the catalysis. The selectivities of DIPB isomers were almost constant during the catalysis, and the selectivities for IPBP isomers decreased slightly with an increase in that for TriIPB isomers. These results show that the formation of DIPB and IPBP isomers occurred inside the pores, and the products formed inside the pores rapidly diffused out. The product distribution of the encapsulated products shows that the catalysis steadily occurs inside pores.

Figure 11 shows the influences of reaction period on the selectivities for IPBP and DIPB isomers in bulk and encapsulated products in the isopropylation of BP over A_3 zeolite. The influences of the selectivities for IPBP and DIPB isomers in bulk products are shown in Fig. 11a. The selectivities for 4,4′-, 3,4′-, and 3,3′-DIPB were almost constant during the catalysis; however, the selectivity for 4-IPBP decreased with an increase in the selectivity for 3-IPBP. These results suggest that 3-IPBP accumulated because of rapid consumption of the highly reactive 4-IPBP, and that the formation of 4,4′-DIPB occurred predominantly through 4-IPBP. These results mean that "product selectivity" is operated in the catalysis.[1–5] Figure 11b shows the selectivities for 4,4′-DIPB and 4-IPBP were almost constant in the encapsulated products during the catalysis. These results suggest that the AFI channels can discriminate the transition state of 4,4′-DIPB from those of the other isomers resulting in the selective formation of the least bulky 4,4′-DIPB. It is worthy to note that the selectivity for

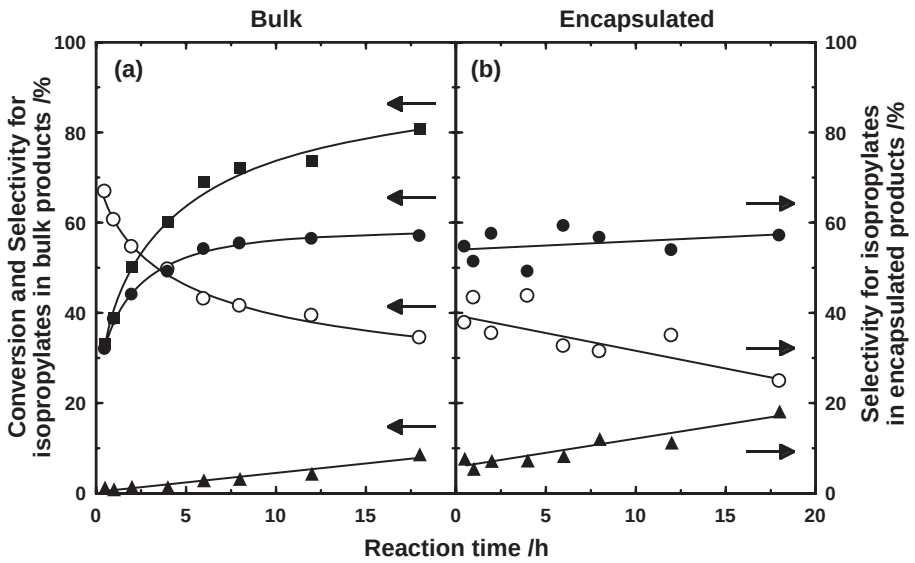

Fig. 10. The influence of reaction time on the selectivity for isopropylates in the isopropylation of BP over H-[Al]-SSZ-24 zeolite. (a) Conversion and yield of isopropylates in bulk products. (b) Composition of isopropylates in encapsulated products. Reaction conditions: zeolite: A_3, 0.25 g; BP, 50 mmol; propene: 0.8 MPa; temperature: 175 °C. Legends: ■, conversion. ●, DIPB; ○, IPBP; ▲, TriIPB.

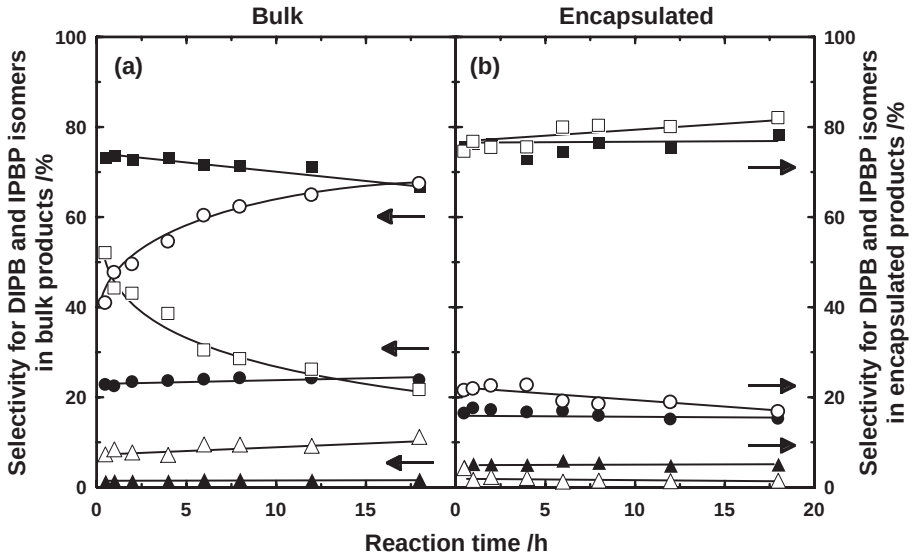

Fig. 11. The influence of reaction time on the selectivity for IPBP and DIPB isomers in the isopropylation of BP over H-[Al]-SSZ-24 zeolite. (a) Selectivity for IPBP and DIPB isomers in bulk products. (b) Selectivity for IPBP and DIPB isomers in encapsulated products. Reaction conditions: see Fig. 10. Legends: DIPB isomers: ■, 4,4′-; ●, 3,4′-; ▲, 3,3′-. IPBP isomers: □, 4-; ○, 3-; △, 2-.

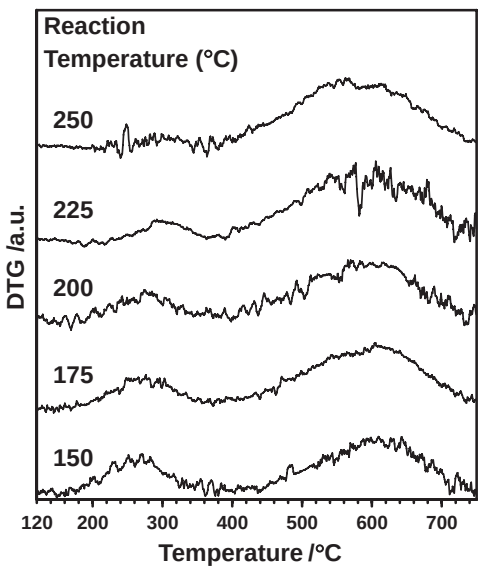

Fig. 12. The influence of reaction temperature on TG profiles of the zeolite used for the isopropylation of BP. Reaction conditions: see Fig. 8.

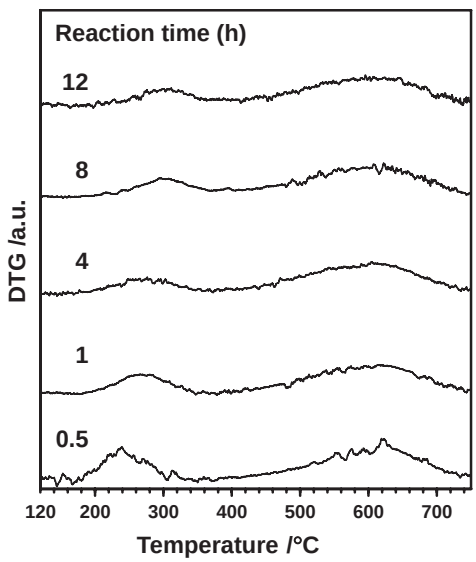

Fig. 13. The influence of reaction time on TG profiles of the zeolite used for the isopropylation of BP. Reaction conditions: see Fig. 10.

4-IPBP among IPBP isomers was as high as 80% in the encapsulated products during the catalysis. These results mean that the products rapidly diffuse inside the channels and that the shape-selective catalysis steadily occurs. The less bulky 4-IPBP can be accommodated easier than 3-IPBP inside channels, and thus, predominantly isopropylated to 4,4′-DIPB inside the channels. Similar exclusion of 3-IPBP was observed during the isopropylation of BP over H-MOR.[10]

The TG profiles of the zeolites used for the reactions are shown in Figs. 12 and 13. Figure 12 shows the influences of reaction temperature over A_3 zeolite. Coke appeared on the zeolite used for the reaction even at 150 °C: the peaks at 200–300 °C are assigned to encapsulated products and the peaks at 500–600 °C to coke. The amounts of coke gradually increased at higher temperature, and encapsulated products disappeared. These results suggest that the channels of H-[Al]-SSZ-24 zeolites were gradually choked by the coke-deposition, and organic chemicals cannot come out of the channels by heating the zeolites for TG measurements. Figure 13 shows the influences of reaction time on coke formation over A_3 zeolite at 175 °C. Coke appeared just after the reaction started; however, the amount of coke was almost constant during the catalysis. From these results, coke formation inside the channels was not severe towards the isopropylation of BP because acid sites are highly dispersed in the zeolites. Similar results were also observed in the isopropylation over highly dealuminated H-MOR.[3–8]

The *s*- and *t*-Butylation of BP over H-[Al]-SSZ-24 Zeolites. Figure 14 shows the influences of reaction temperature

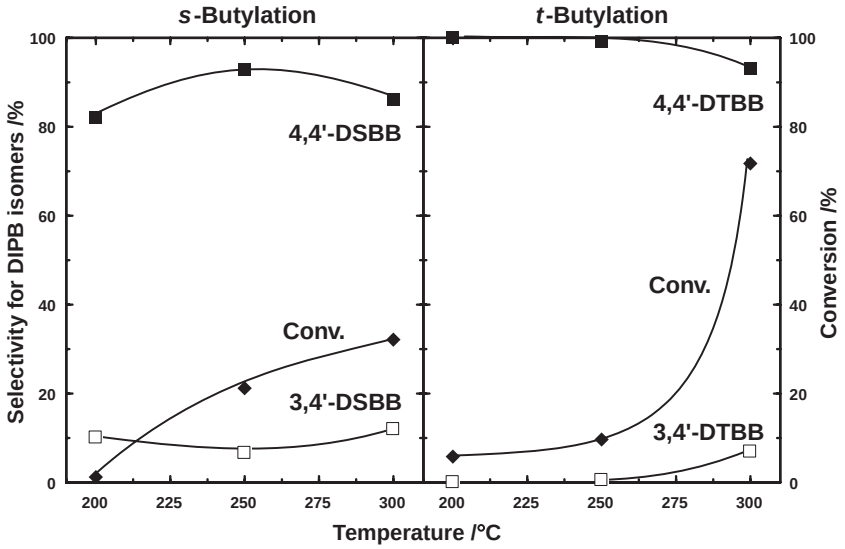

Fig. 14. The selectivity for 4,4′-di-*s*-butylbiphenyl and 4,4′-di-*t*-butylbiphenyl in the *s*- and *t*-butylations of BP. Reaction conditions: zeolite, A_3, 0.125 g; BP, 25 mmol; 1-butene or 2-methylpropene, 0.4 MPa; temperature, 200–300 °C; period, 4 h.

on catalytic activity and the selectivity for 4,4′-di-*s*-butylbiphenyl (4,4′-DSBB) and 4,4′-di-*t*-butylbiphenyl (4,4′-DTBB) in the *s*- and *t*-butylations of BP over A_3 zeolite. Although the catalytic activities were low, *s*- and *t*-butylations of BP yielded selectively the least bulky products, 4,4′-DSBB and 4,4′-DTTB, and the selectivities in the butylations were higher than those in the isopropylation. The difference in the selectivity for 4,4′-dialkylbiphenyl is due to the difference in steric constraints of transition states inside the channels.

Shape-Selective Catalysis over H-[Al]-SSZ-24 Zeolites. Catalytic performances of zeolites for the shape-selective catalysis are generally influenced by many factors.[1,2] Some of typical factors on zeolites are pore structure, and physical properties, such as crystal size, morphology, and density and distribution of active species, which are also influenced by preparation and post-synthesis methods. Reaction conditions, such as temperature, pressure, period, and catalyst amount, also influence the catalytic performances. Among these factors, the pore structure is the most important for controlling the shape-selectivity of the catalysis. The selectivity for the least bulky isomer should be controlled by steric allowance of zeolite pores for transition states to form each isomer.

The shape-selective formation of 4,4′-DIPB was observed in the isopropylation of BP over H-[Al]-SSZ-24 zeolites, which means that AFI channels can accommodate the transition states for 4,4′-DIPB and discriminate among the transition states for the least bulky 4,4′-DIPB and the other isomers. However, the selectivity for 4,4′-DIPB over H-[Al]-SSZ-24 zeolites was lower than that of H-MOR. The difference in the selectivity between the zeolites reflects the difference of twelve-membered pore structures: 0.72×0.72 nm for H-[Al]-SSZ-24 with straight channel and 0.67×0.72 nm for H-MOR with straight channels with side pocket.[16] The formation of bulky DIPB isomers should occur inside the H-[Al]-SSZ-24 zeolite because their channels allow the bulky transition states resulting in lower selectivity for 4,4′-DIPB. The selectivity for 4,4′-DIPB was in the same level as those of SAPO-5 and SSZ-31 zeolites of twelve-membered pore with straight channel and CIT-5 zeolites of fourteen-membered pore with slightly corrugated channel. The differences in pore size reflect the lack of discrimination among the transition states resulting in the lower selectivity for 4,4′-DIPB. These molecular sieves have straight channel with similar pore entrance: 0.72×0.72 nm for SAPO-5,[16] 0.56×0.82 nm for H-[Al]-SSZ-31,[22] and 0.72×0.75 nm for CIT-5.[16]

The selectivity for 4,4′-DIPB in encapsulated DIPB isomers over H-[Al]-SSZ-24 zeolite was influenced by the SiO_2/Al_2O_3 ratio, i.e. the amounts of acid sites. The selectivity decreased at higher temperatures during the isopropylation of BP over the zeolites with high acid amounts. In these zeolites, the isomerization of 4,4′-DIPB occurs at internal acid sites because the channels are large enough to allow the isomerization of 4,4′-DIPB. However, the isomerization of 4,4′-DIPB did not occur inside the channels of H-[Al]-SSZ-24 zeolites with high SiO_2/Al_2O_3 ratio, whereas a decrease in the selectivity for 4,4′-DIPB in the bulk products was observed due to isomerization at external acid sites. From these considerations, we can conclude that the internal and external acid sites of H-[Al]-SSZ-24 zeolites are active in the isomerization of 4,4′-DIPB resulting in the decrease in the selectivity for 4,4′-DIPB in the isopropylation of BP. These features over H-[Al]-SSZ-24 zeolites are quite different from those of H-MOR: no isomerization occurred inside the pore of H-MOR because of the steric restriction.[3–8] A similar decrease in the selectivity for 4,4′-DIPB occurred for MAPO-5 (M: Mg and Zn) with AFI topology.[13–15] However, no isomerization of 4,4′-DIPB was found in the encapsulated products for SAPO-5 although it has AFI topology.[9] This may be due to its weak acidity.[23]

There is another mechanism for the decrease in the selectivity for 4,4′-DIPB in the encapsulated products due to the change of pore structure of H-[Al]-SSZ-24 zeolites. A fluctuation in the channel width at higher temperatures could cause a decrease in the steric restriction of the transition state to form 4,4′-DIPB resulting the decrease in the shape-selective nature of H-[Al]-SSZ-24 zeolites. However, this mechanism is not probable because A_1 zeolite had high selectivity for 4,4′-DIPB

even at 300 °C and because the isomerization of 4,4′-DIPB did not occur even at 325 °C.

The selectivity for the least bulky 4,4′-dialkylbiphenyl were increased in the order: 4,4′-DIPB < 4,4′-DSBB < 4,4′-DTBB. These differences reflect the differences in steric constraint at the transition states inside the channels, and the predominance of the least bulky products increases with the bulkiness of the alkylating agent.

Conclusion

H-[Al]-SSZ-24 zeolites with AFI topology were synthesized from [B]-SSZ-24 zeolites, and applied for the alkylation of BP. The alumination enhanced the catalytic activity. Shape-selective formation of 4,4′-DIPB occurred at moderate temperature; however, the selectivity for 4,4′-DIPB decreased with an increase in the reaction temperature. Isomerization of 4,4′-DIPB occurred at higher temperatures over internal and external acid sites of the zeolites when there are enough acid sites inside the channels. However, no isomerization was obserbed inside the channels of the zeolite with high SiO_2/Al_2O_3 ratio although isomerization occurred at the external acid sites. These results suggest that the AFI channels can discriminate 4,4′-DIPB from the other DIPB isomers at their transition states and that the channels allowed the isomerization of 4,4′-DIPB at higher temperatures.

H-[Al]-SSZ-24 zeolites gave lower selectivity for 4,4′-DIPB than H-MOR zeolites. These differences of H-[Al]-SSZ-24 zeolites and H-MOR are due to the pore structures. The former zeolite has a slightly larger channels than the latter, and the discrimination of the transition states of 4,4′-DIPB from other bulkier isomers by the former zeolite is looser than that by the latter.

The *s*- and *t*-butylations of BP yielded almost selectively the least bulky products, 4,4′-DSBB and 4,4′-DTTB over H-[Al]-SSZ-24 zeolites, and the selectivities were higher than those of the isopropylation. These differences in the selectivity for 4,4′-dialkylbiphenyl show that the shape-selective catalysis occurred inside the channels, and governed by steric constraints of transition states.

Further aspects on the influences of the shape-selective catalysis on the zeolite structures are under investigation. The details will be discussed in near future.

A part of this work was financially supported by a Grant-in-Aid for Scientific Research (B) Nos. 15350093 and 16310056, the Japan Society for the Promotion of Science (JSPS). Y. K. thanks the Core Research for Evolution Science and Technology (CREST) of Japan Science and Technology Corporation (JST).

References

1 S. M. Csicsery, *Zeolites* **1984**, *4*, 202.
2 P. B. Venuto, *Microporous Mater.* **1994**, *2*, 297.
3 Y. Sugi, Y. Kubota, *Catalysis, Specialist Periodical Report*, ed. by J. J. Spivey, Royal Soc. Chem. Cambridge, U.K., **1997**, Vol. 13, pp. 55–84.
4 Y. Sugi, K. Komura, J.-H. Kim, *J. Korean Ind. Eng. Chem.* **2006**, *17*, 235.
5 Y. Sugi, Y. Kubota, T. Hanaoka, T. Matsuzaki, *Catal. Surv. Jpn.* **2001**, *5*, 43.
6 T. Matsuzaki, Y. Sugi, T. Hanaoka, K. Takeuchi, H. Arakawa, T. Tokoro, G. Takeuchi, *Chem. Express* **1989**, *4*, 413.
7 Y. Sugi, T. Matsuzaki, T. Hanaoka, Y. Kubota, J.-H. Kim, X. Tu, M. Matsumoto, *Catal. Lett.* **1994**, *27*, 315.
8 Y. Sugi, S. Tawada, T. Sugimura, Y. Kubota, T. Hanaoka, T. Matsuzaki, K. Nakajima, K. Kunimori, *Appl. Catal., A* **1999**, *189*, 251.
9 R. K. Ahedi, S. Tawada, Y. Kubota, Y. Sugi, J. H. Kim, *J. Mol. Catal. A* **2003**, *197*, 133.
10 Y. Sugi, T. Sugimura, S. Tawada, Y. Kubota, *Catal. Lett.* **2001**, *77*, 159.
11 Y. Kubota, S. Tawada, C. Naitoh, K. Nakagawa, N. Sugimoto, Y. Fukushima, Y. Sugi, *Shokubai* **1999**, *41*, 380.
12 M. Bandyopadhyay, R. Bandyopadhyay, S. Tawada, Y. Kubota, Y. Sugi, *Appl. Catal., A* **2002**, *225*, 51.
13 S. K. Saha, S. B. Waghmode, H. Maekawa, K. Komura, Y. Kubota, Y. Sugi, Y. Oumi, T. Sano, *Microporous Mesoporous Mater.* **2005**, *81*, 289.
14 S. K. Saha, H. Maekawa, S. B. Waghmode, S. A. R. Mulla, K. Komura, Y. Kubota, Y. Sugi, S.-J. Cho, *Mater. Trans.* **2005**, *46*, 2659.
15 H. Maekawa, S. K. Saha, S. A. R. Mulla, S. B. Waghmode, K. Komura, Y. Kubota, Y. Sugi, *J. Mol. Catal. A: Chem.* **2006**, *263*, 238.
16 IZA Structure Commission: http://www.iza-structure.org/databases/.
17 S. I. Zones, U. S. Patent 4,665,110, **1987**.
18 S. I. Zones, Y. Nakagawa, *Microporous Mater.* **1994**, *2*, 557.
19 R. F. Lobo, M. E. Davis, *Microporous Mater.* **1994**, *3*, 61.
20 Y. Kubota, S. Tawada, K. Nakagawa, C. Naitoh, N. Sugimoto, Y. Fukushima, T. Hanaoka, Y. Imada, Y. Sugi, *Microporous Mesoporous Mater.* **2000**, *37*, 291.
21 C. Fild, H. Eckert, H. Koller, *Angew. Chem., Int. Ed.* **1998**, *37*, 2505.
22 R. F. Lobo, M. Tsapatsis, C. C. Freyhardt, I. Chan, C. Y. Chen, S. I. Zones, M. E. Davis, *J. Am. Chem. Soc.* **1997**, *119*, 3732.
23 M. Hartman, L. Kevan, *Res. Chem. Intermed.* **2005**, *28*, 625.